A framework for getting the correct T_2 distribution from multiple echo magnitude MRI signal

Ruiliang Bai[1,2], Cheng Guan Koay[3], and Peter J Basser[1]

[1]Section on Tissue Biophysics and Biomimetics, PPITS, NICHD, National Institutes of Health, Bethesda, MD, United States, [2]Biophysics Program, Institute for Physical Science and Technology, University of Maryland, College Park, MD, United States, [3]Department of Medical Physics, University of Wisconsin School of Medicine and Public Health, Madison, WI, United States

Target Audience: Clinicians and basic scientists who are interested in quantitative T_2 relaxation methods and noisy signal correction in magnitude MRI.

Introduction: Quantitative T_2 (qT_2) MRI has attracted more attention in recent years due to its ability to identify microstructure-dependent T_2 components empirically, without prior modeling asssumptions.[1] Typically, a single slice multi-echo acquisition is performed and then the magnitude data is directly fitted with an inverse Laplace transform (ILT) algorithm to obtain the T_2 distribution. However, this noisy magnitude data is subject to Rician distribution, rather than Gaussian distribution, which can produce artifacts in conventional ILT algorithms, that implicitly assume the signal is always Gaussian distributed.[2,3] These artifacts include generation of non-existing CSF-like long T_2 components, biasing the true geometric mean T_2 (gmT_2) values and the relative fractions of various components, and blurring nearby T_2 peaks.[3] Here we propose a framework to map noisy Rician-distributed magnitude MRI signal back to a Gaussian distribution and then to perform an ILT algorithm on the corrected data to obtain an accurate T_2 distribution.[4] Both simulations and experiments validate this approach.

Methods: The proposed framework includes three steps: 1. Estimation of the noise variation (standard deviation) from the multi-echo MRI magnitude data;[5] 2. A signal transformational framework developed previously [4,6] was modified and used to correct Rician distributed magnitude data in each voxel to Gaussian distributed data; 3. Employing a non-negative least square (NNLS) algorithm with Tikhonov regularization on the corrected signal to obtain the T_2 distribution for each voxel. Simulations were performed on both single T_2 component and double T_2 components with various noise levels. In each simulation, 200 realizations with random Gaussian noise on both real and imaginary channels were generated and the averaged distributions were used for comparison. Multiple echo spin-echo acquisitions were performed on a 7 T Bruker Advance III MRI scanner equipped with a micro2.5 gradient system. A single slice was acquired (TR/TE = 3000ms/7ms, 128x128, 1.00mm thickness, FOV 12mm×12mm) through a fixed porcine spinal cord with 64 repetitions.

Results and Discussions:

Fig 1: A. Example of corrected and uncorrected spectra. B. Simulations with SNR for a single T_2 component and C. two T_2 components.

(1) Simulation:
Fig 1A shows an example of how well the signal transformation works. Before the correction, there is an offset in the magnitude MRI signal when the underlying signal is approaching zero, which is reflected in the T_2 spectrum as a tail in the long relaxation time regime. This shifts the main peak to occur at a shorter relaxation time. After correcting magnitude signal and re-performing the NNLS, the spurious tail at the longer relaxation times disappears and the position of the main peak ($T_2 \approx 50$ms) is corrected. The corresponding fit obtained from the corrected T_2 spectrum is closer to the ground truth. In Fig 1B these artifacts motioned above were systematically studied as a function of the initial SNR. Before correction (upper), the estimated fraction of the longer tail component and the shift of the main peak worsen as SNR goes down. However, after correction (lower), the T_2 spectrum is more consistent over the entire range of SNRs. Similar results are obtained for the more challenging problem of two relaxation components with relaxation times and weights given by (T_2, weight) = (25ms, 50%) and (60ms, 50%). Another important improvement is that the blurring of the two components caused by noise in the magnitude data was significantly corrected by the proposed framework: the two components become visible and their positions and fractions are closer to the underlying ground truth.
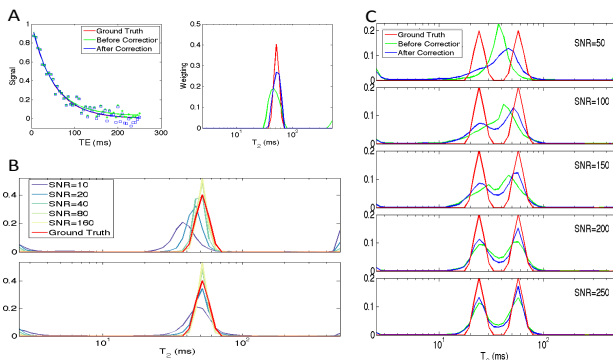
(2) Experiments: The 64 repetitions were randomly assembled to achieve 1, 2, 4, 8, 16, 64 averages. The corresponding initial SNR for white matter is 30, 42, 60, 85, 120, 240 and the gray matter is around 1.5 times higher than white matter. The 64 signal averaged results were taken as the ground truth here. In Fig 2A it is the image of gmT_2 (ms) of the whole T_2 distribution with 64 averaging. Fig 2B shows that the fraction of the tails on the longer relaxation time regime was significantly corrected through the entire SNR range. Two ROIs in white matter and one ROI in gray matter with relatively homogenous gmT_2 were selected for further analysis. The spectrums of all the voxels before (left) and after (right) correction in each ROI were averaged and shown in Fig 2C 1-3. In both ROIs 1 and 2, the correction made the two peaks visible even at the lowest SNR=30, and the positions and fractions of the two components returned to the ground truth faster as SNR increases. In ROI 3, the underlying T_2 spectrum has single peak with a broad distribution. Our framework successfully corrected the left shift of the main component and also made the shape of the distribution closer to the ground truth for the entire SNR range.

Conclusions: Our simulations and experimental results demonstrated that using our proposed framework can significantly correct artifacts in the T_2 distribution caused by Rician-distributed magnitude data, including the CSF-like long T_2 components, shifts of the main T_2 component, and the blurring of two nearby distinct T_2 components. More importantly, the effect of the correction is more obvious in the low SNR regime, which makes the method more practical for clinical multi-echo MRI data.
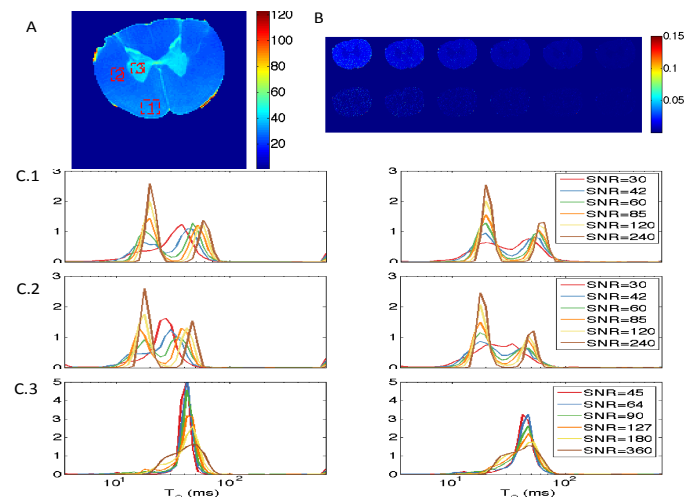

Fig 2: A. The gmT_2 map of the spinal cord. B. The fraction map of the $T_2 > 200$ms components before correction (upper) and after correction (lower) with various SNR (left to right, 1, 2, 4, 8, 16, 64 averaging). C. 1-3: The T_2 spectrum of the ROI 1-3 before (left) and after (right) correction.

References: 1. A. MacKay, C. Laule, I. Vavasour, T. Bjarnason, S. Kolind, and B. Mädler, *Magn. Reson. Imaging*, 2006, **24**, 515–525. 2. H. Gudbjartsson and S. Patz, *Magn. Reson. Med.*, 1995, **34**, 910–914. 3. T. A. Bjarnason, C. Laule, J. Bluman, and P. Kozlowski, *J. Magn. Reson.*, 2013, **231**, 22–31. 4. C. G. Koay, E. Özarslan, and P. J. Basser, *J. Magn. Reson.*, 2009, **197**, 108–119. 5. C. G. Koay, E. Özarslan, and C. Pierpaoli, *J. Magn. Reson.*, 2009, **199**, 94–103.6. C. G. Koay and P. J. Basser, *J. Magn. Reson.*, 2006, **179**, 317–22.